JOURNAL OF AGRICULTURAL AND FOOD CHEMISTRY

J. Agric. Food Chem. **2009,** *57,* 1903–1907 **1903**

Initial Studies on the Quantitation of Bruise Damage and Freshness in Mushrooms Using Visible-Near-Infrared Spectroscopy

CARLOS ESQUERRE,*,†,‡ AOIFE A. GOWEN,‡ COLM P. O'DONNELL,‡ AND GERARD DOWNEY†

Teagasc, Ashtown Food Research Centre, Ashtown, Dublin 15, Ireland, and Biosystems Engineering, School of Agriculture, Food Science and Veterinary Medicine, University College Dublin, Dublin 4, Ireland

Identification of mushrooms that have been physically damaged and the measurement of time elapsed from harvest are very important quality issues in industry. The purpose of this study was to assess whether the chemical changes induced by physical damage and the aging of mushrooms can: (a) be detected in the visible and near infrared absorption spectrum and (b) be modeled using multivariate data analysis. The effect of pre-treatment and the use of different spectral ranges to build PLS models were studied. A model that can identify damaged mushrooms with high sensitivity (0.98) and specificity (1.00), and models that allow estimation of the age (1.0-1.4 days root mean square error of cross-validation) were developed. Changes in water matrix and alterations caused by enzymatic browning were the factors that most influenced the models. The results reveal the possibility of developing an automated system for grading mushrooms based on reflectance in the visible and near infrared wavelength ranges.

KEYWORDS: Chemometrics; visible-NIR spectroscopy; mushrooms; enzymatic browning; *Agaricus bisporus*

INTRODUCTION

Mushrooms (*Agaricus bisporus)* have been consumed as a food delicacy since early times (*1, 2*). Nowadays, they are an important agricultural commodity produced in Ireland on a commercial basis since the mid-1930s. Since then, annual production has increased up to 77×10^3 t with an export value of US $136.5 million in 2005 (*3*).

Mushrooms are delicate foodstuffs and can be easily bruised by physical stress during harvesting, handling, and transportation; this mechanical damage triggers a browning process, which is the main cause of value loss in the market (*4, 5*). Another relevant factor in mushroom quality is the elapsed time between harvesting and the time of reaching the market. This is of particular importance for an exporting country such as Ireland for which access to food markets in larger, neighboring countries within Europe is vital.

Therefore, development of a relatively simple, objective, and nondestructive method to (a) identify physical damage before damage-induced browning becomes visible and (b) quantify the postharvest age of mushrooms is of strategic importance to the Irish mushroom industry.

NIR spectroscopy has proved to be one of the most efficient and advanced tools for continuous monitoring and controlling of process and product quality in the food processing industry over the past three decades (*6*−*10*). Critical to the effective deployment of this technique is the availability of powerful mathematical tools for the interrogation and mining of large spectral data sets. Partial least-squares (PLS) regression and discriminant analysis are two powerful chemometric tools that have been used for this purpose in food applications (*11*−*14*); they are studied in the present article to (a) differentiate between damaged and undamaged mushrooms and (b) to determine mushroom freshness.

MATERIALS AND METHODS

Mushrooms. A set of 168 closed cap, defect-free *Agaricus bisporus* strain Sylvan A15 (Sylvan Spawn Ltd., Peterborough, United Kingdom) mushrooms (3−5 cm cap diameter) were selected for this study. They were second flush mushrooms grown at the Teagasc Research Centre Kinsealy (Dublin, Ireland) in a manner typical of the mushroom industry, harvested in the normal manner, and transported by road immediately afterward to the laboratory in Ashtown Food Research Centre (Dublin, Ireland). Elapsed time between harvest and delivery to Ashtown was approximately 3 h; special cardboard trays, designed to hold 48 mushrooms by the stem using a metal grid to avoid contact between (a) mushrooms and (b) between the top of mushrooms caps and the tray lid, were used for this transportation.

Treatments. A subset of 84 mushrooms was subjected to physical damage using a mechanical shaker (Gyrotory G2, New Brunswick Scientific Co. USA) set at 300 rpm for 10 min; these samples were labeled as damaged (D). The remaining samples (84) were labeled as

* Corresponding author. E-mail: carlos.esquerre@teagasc.ie.
† Teagasc.
‡ University College Dublin.

10.1021/jf803090c CCC: $40.75 © 2009 American Chemical Society
Published on Web 02/12/2009

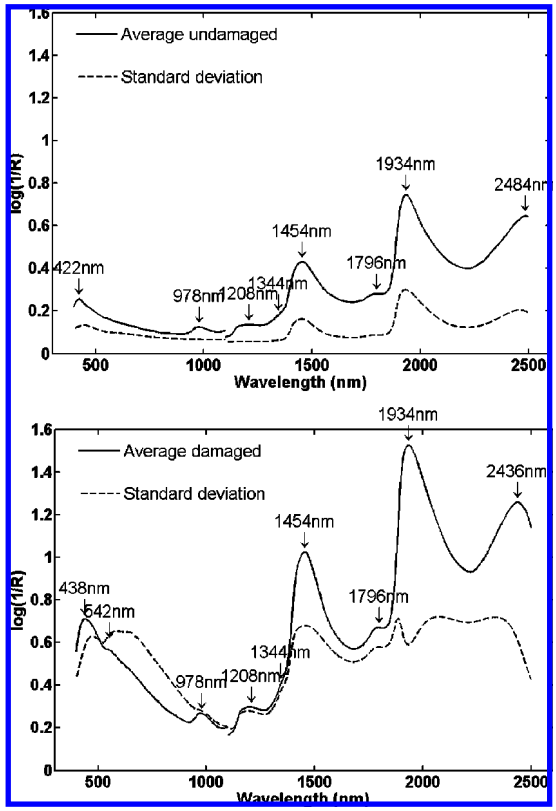

Figure 1. Average and standard deviation raw spectra of damaged and undamaged mushrooms. Standard deviation has been scaled by a factor of 3.

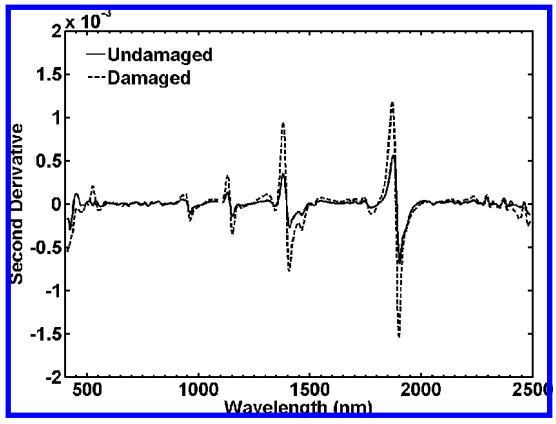

Figure 2. Second derivative of average mushroom spectra using the Savitzky−Golay algorithm (11 point gap, second order polynomial smooth).

undamaged (U). Spectra of 12 undamaged and 12 damaged mushrooms were recorded directly after damage induction. The remainder of the mushrooms (72 each of damaged and undamaged) were placed carefully in plastic punnets (six mushrooms per punnet), covered with plastic film (Lin-Wrap film PVC, LinPac Plastics, Pontivy, France), and stored at two controlled temperatures, i.e., +4 °C (T4) and +15 °C (T15). At each further sampling time (day 3, 6, and 9), 12 damaged and 12 undamaged mushrooms were removed from each storage temperature for spectral collection. All sample handling was carried out with the utmost care to avoid damage to the mushroom samples.

Visible-NIR spectroscopy. Spectra were collected in reflectance mode using a NIRSystems 6500 instrument (Foss NIRSystems, Denmark) equipped with a remote reflectance fiber optic probe (part number NR 6539-A) over the wavelength range 400−2498 at 2 nm intervals. Data were recorded as absorbance (log 1/*R*), converted to JCAMP-DX format (*15*), imported directly into The Unscrambler (v 9.2; CAMO AS, Oslo, Norway), and finally exported as a Matlab file.

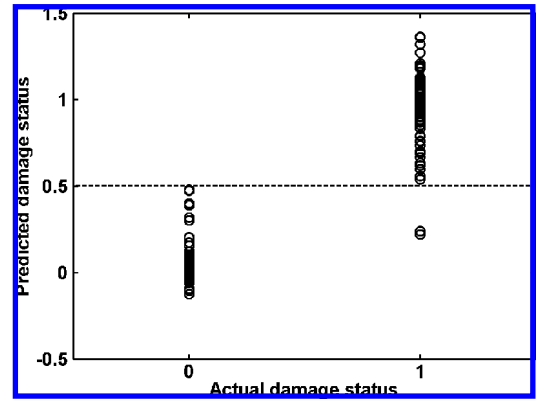

Figure 3. Damage classification of mushrooms based on PLS-DA regression of raw spectra (400−2498 nm range) using 2 latent variables (0 = undamaged; 1 = damaged).

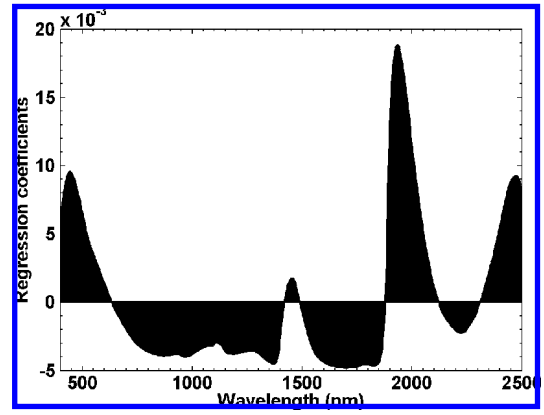

Figure 4. PLS regression coefficients for the classification of mushrooms as damaged or undamaged (PLS-DA model built using two latent variables on raw spectra in the range 400−2498 nm).

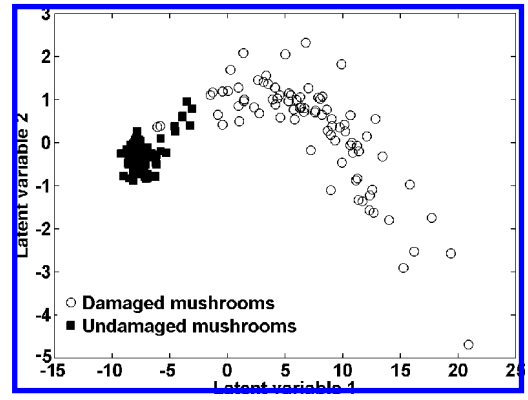

Figure 5. PLS scores plot on latent variables 1 (78% of variance) and 2 (10% of variance) from a discriminant model developed to identify damaged mushrooms.

Two punnets with undamaged mushrooms and two punnets with damaged samples were randomly selected and removed from each storage temperature every day of analysis; samples were allowed to equilibrate to ambient temperature (15−20 °C) before removing the plastic covering, lifting out individual mushrooms, and acquiring the spectra.

Each mushroom was placed upside down on the optical window of the fiber optic probe, and both the sample plus probe were covered with a black cardboard box wrapped in aluminum foil to exclude stray light ingress. After recording a spectrum, the mushroom was rotated on its vertical axis through 90° and a second spectrum collected; the average of both spectra was used in subsequent chemometric analysis.

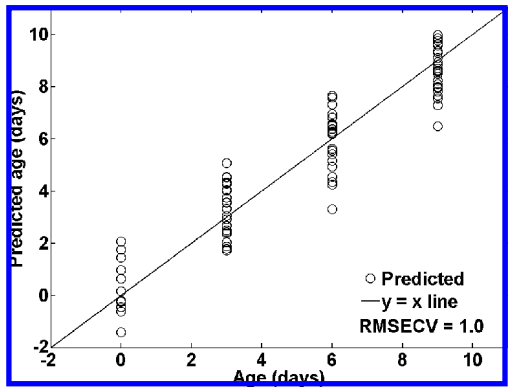

Figure 6. Predicted age of undamaged mushrooms stored at 4 and 15 °C by PLS regression (full cross-validation; 2der, 15 point gap; 400−2498 nm; 9 latent variables).

Table 1. PLS Regressions Models to Predict Age of Mushrooms

damage status	storage temperature	pretreatment (gap points)	range (nm)	RMSECV (day)	R^2	#LV[a]
undamaged	T4-T15	2der(15)	400−2498	1.0	0.89	9
	T4-T15	2der(21)	400−2498	1.9	0.64	9
damaged	T4	1der(19)	400−748	1.3	0.85	6
	T15	1der(19)	400−748	1.4	0.84	6

[a] #LV: number of latent variables.

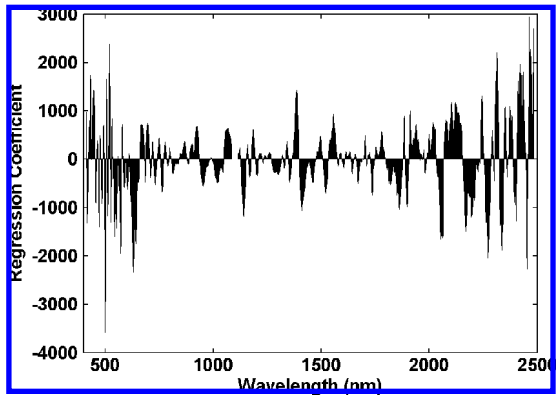

Figure 7. Regression coefficients for the PLS model of age in undamaged mushrooms (2der; 15 point gap; 9 latent variables; range 400−2498 nm; 4° and 15 °C storage temperature).

Chemometrics. Prior to the development of multivariate models for damage and age prediction, four pretreatments were separately applied to the spectra: these were standard normal variate (SNV), multiplicative scatter correction (MSC), first derivative (1der), and second derivative (2der) Savitzky−Golay. In the case of the derivative pretreatments 3, 5, 7, 9, 11, 13, 15, 17, 19, and 21, data point gaps followed in each case by a second order polynomial smoothing step were studied (*16*−*20*). To identify wavelength regions containing the most information with respect to damage and age, four ranges were studied, i.e., 400−748 nm (visible), 750−1098 nm, 1100−2498 nm, and 400−2498 nm. The rationale for this was to (a) reduce the number of datapoints while maintaining accuracy, this increases the possibility of calibrations being robust, and (b) to allow for the possibility of cheaper NIR instruments being used since such instruments typically only scan a subset of the visible-NIR range.

Partial least-squares regression (*21*−*23*) was applied to the centered spectral data sets to develop separate models for damage (partial least-squares discriminant analysis (PLS-DA) classification model) and prediction of postharvest age (partial least-square regression (PLSR) calibration model). Models were optimized by the use of leave-one-out (i.e., full) cross-validation given that sample numbers available were small; prediction statistics were recorded for the optimum model. In total, in the case of damage estimation, combinations of the factors studied, i.e., temperature (T4, T15, and T4+T15), wavelength range (400−2498 nm, 1100−2498 nm, 750−1498 nm, and 400−748 nm), and spectral pretreatment (none, SNV, MSC, 1der, and 2der), were examined. Partial least-squares discriminant analysis (PLS-DA) (*12*, *24*, *25*) was applied to develop qualitative models for distinguishing between damaged and undamaged mushrooms. For this purpose, a dummy *Y*-variable was assigned to each mushroom sample, 0 for undamaged and 1 for damaged. Using a somewhat arbitrary but not unreasonable cutoff value of 0.5, samples with a predicted dummy variable <0.5 were identified as belonging to class 0, while those with predicted *Y*-values ≥ 0.5 were classified as belonging to class 1. Performance of these classification models was evaluated on the basis of their sensitivity (number of samples of a given type correctly classified as that type) and specificity (number of samples not of a given type correctly classified as not of that type) (*12*, *26*), and the number of latent variables (#LV) required by each.

To find the most accurate models for the prediction of mushroom age, PLSR calibration models, developed with leave-one-out cross-validation, were built for the combinations of the factors studied, i.e., damage (U, D, and U+D), temperature (T4, T15, and T4+T15), wavelength range (400−2498 nm, 1100−2498 nm, 750−1498 nm, and 400−748 nm), and spectral treatment (none, SNV, MSC, 1der, and 2der). Performance of the age prediction models was evaluated using the root-mean-square error of cross-validation (RMSECV), coefficient of determination (R^2), and number of latent variables required (#LV).

RESULTS AND DISCUSSION

Spectra. The average absorption spectra of the 84 damaged and 84 undamaged mushrooms analyzed are shown in **Figure 1**; also included in these figures are the standard deviation spectra associated with these means. The highest average absorbance is around 1.5 absorbance units, well within the linear photometric range of the instrument detector (*27*). The peaks at 1934, 1454, 1208, and 978 nm are attributed mainly to vibrational absorptions of water. Shoulders present at 1796 and 1344 nm could be related to the second and third overtones of −C═O stretching of anhydrides (*28*, *29*). Examination of the standard deviation spectra at each wavelength, which reflect the positions of major variability in the spectral collection, shows clearly that the positions of major variability do not coincide exactly with the major absorbance peaks but rather are located on the shoulder of these features. Variation in mushroom color is evidenced by the standard deviation plot between 400 and 750 nm, the visible wavelength range. The average spectrum of damaged mushrooms shows greater absorbance than is the case for undamaged mushrooms especially in the water-related peaks; this may indicate that water was released from internal structures as a result of the physical damage. Differences in the visible region (peaks at 438 and 542 nm) are due to the formation of pigmented compounds, mainly melanins, which are not homogeneous compounds and which can produce colors varying from yellow to red (*30*, *31*). Second derivative average spectra, shown in **Figure 2**, reveal greater spectral detail as expected; here again, it is obvious that the locations of maximum spectral variance do not coincide with regions of maximum absorbance. In the particular case of the second derivative spectra, this data pretreatment resolves the broad maxima seen in raw spectral plots into a number of sharper peaks (*32*). Interpretation of the second derivative is somewhat easier than is the case for raw spectra because of these sharper and nonoverlapping features. It is also notable that there appears to be some spectral information present above 2200 nm in this figure that could be related to combinations of -CH and -CC-, and aromatic -CH bonds (*28*, *29*).

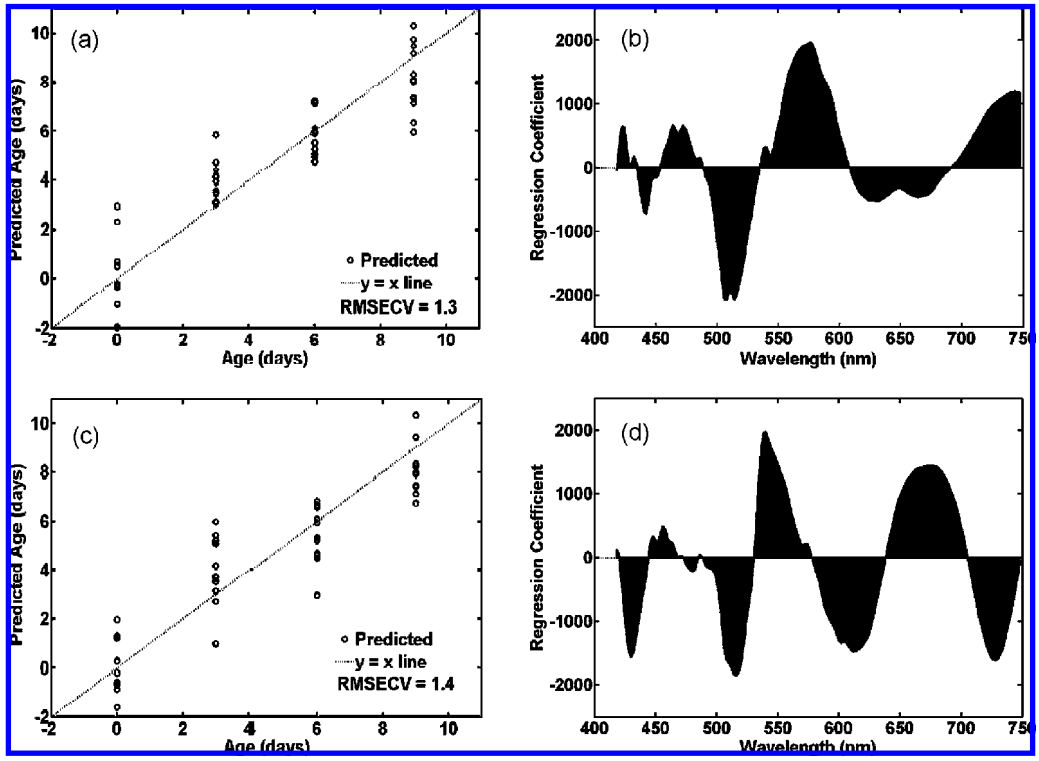

Figure 8. PLS regression plots of predicted age of damaged mushrooms by full cross-validation (first derivative; 19 point gap; 400−748 nm; 6 latent variables) stored at 4 °C: (**a**) Predicted age; (**b**) Regression coefficients. Stored at 15 °C: (**c**) Predicted age; (**d**) Regression coefficients.

Modeling Physical Damage. Perfect classification (sensitivity = 1.00 and specificity = 1.00) in the case of mushrooms stored at 4 °C was achieved by the application of PLS-DA to either raw or SNV preprocessed spectra in the range 750 to 1098 nm. In the case of mushrooms stored at 15 °C, perfect classification was achieved using raw or SNV preprocessed spectra in the wavelength range 400−2498 nm and for MSC preprocessed spectra in the ranges 400−2498 nm and 750−1098 nm. However, the large number of latent variables (#LV = 16−22) required for these models suggests an overfitting of the model to the data set with the resulting incorporation of noise in the model (*32*, *33*). For these reasons, the preferred classification model involved two latent variables and was developed from untreated spectra over the range 400−2498 nm of mushrooms stored at both temperatures combined into a single data set. Almost all (82 out of 84) damaged mushrooms were recognized as damaged (sensitivity = 0.98), while no undamaged mushroom was misclassified as damaged (specificity = 1.00); the overall correct classification for this model was 99% (**Figure 3**). A visual analysis of the two misclassified samples, one stored at 15 °C for 3 days and the other one stored at 4 °C for 6 days, revealed that the intensity level of injury observed in both samples was less pronounced than that observed for the remainder of the same storage-temperature sample group.

Regression coefficients for the selected classification model are shown in **Figure 4**. It can be observed that the largest peak corresponds to 1934 nm, which may be attributed to changes in water absorption associated with tissue damage by cytoplasm breakdown, releasing vacuolar and vesicular contents increasing the free water. The second greatest peak (444 nm) may be associated with brown pigments formed in the injured tissue, while the third major band at 2474 nm may be associated with the second overtone of O−H stretching of phenols (*29*); this peak could be explained by the activation of tyrosinase present in mushrooms, which catalyzes the oxidation of phenolics to quinones, which, in turn, undergo further oxidation and polymerization reactions to produce the brown pigments characteristic of damaged mushrooms (*34*, *35*). A PLS score plot for all samples on latent variables 1 and 2 of this model is shown in **Figure 5**; these latent variables accounted for 78% and 10%, respectively, of the variability of the damaged mushroom spectral data set. This figure reveals that undamaged mushrooms form a relatively discrete cluster, while damaged mushrooms are more dispersed in this particular two-dimensional space as might be expected given the variation in age and therefore extent of damage in the latter class.

These results show the feasibility of developing an automatic classification system of mushrooms as either damaged or undamaged using visible-NIR spectra and chemometrics that could be implemented in industry.

Modeling Age. The most accurate models for identifying the postharvest age of mushrooms in this study are shown in **Table 1**. The age of undamaged mushrooms could be predicted with a level of accuracy, which may be commercially useful by a second derivative pretreatment (**Figure 6**); corresponding regression coefficients are shown in **Figure 7**. There are common processes involved in senescence at both temperatures (4 and 15 °C) that affect the visible and NIR range of the spectra. The regression coefficients in the visible range present high variability (**Figure 7**); this could be explained by variations in color arising from absorptions by substrates and products of enzymatic browning that absorb in this range of the spectra (*34*). In the NIR region, the most significant regression coefficients are found at 2482 and 2304 nm. While absorption at the former may be associated with O−H stretching of phenols, absorption at 2304 nm could arise from the second overtone of C═C bond stretching in an aromatic ring structure. Both structures are related to the development of enzymatic browning. Significant regression coefficients are also located at 2440, 2016, and 1960 nm; the attribution of these peaks is not clear to us. The aging process in damaged mushrooms is best modeled if the storage

temperature is taken into account, i.e., if separate models are developed for 4 and 15 °C storage temperatures. Best models were generated by applying a first derivative (19 points gap) to spectra recorded in the visible range (400−748 nm) employing 6 latent variables (**Figure 8**). Cap discoloration in damaged mushrooms is the main change associated with the aging process. The main difference in regression coefficients between damaged mushrooms stored at 4 °C and those stored a 15 °C was a peak between 632 and 702 nm; the attribution of this peak is unknown.

These results reveal that chemical changes induced by mechanical bruising and the aging of mushrooms could be successfully identified and followed by visible and infrared spectroscopy, and modeled by appropriate chemometric tools. Consequently, the application of visible and NIR spectroscopy could enable the development of a relatively simple, automatic, and online method to (a) identify those mushrooms that have been physically damaged and (b) quantify the postharvest age of mushrooms for the benefit of the mushroom industry and retail sector, respectively.

LITERATURE CITED

(1) Chang, S.; Miles, P. G. The Nutritional Attributes of Edible Mushrooms. In *Mushrooms: Cultivation, Nutritional Value, Medicinal Effect, and Environmental Impact*, 2nd ed.; CRC Press: Boca Raton, FL, 2004; p 2.

(2) Kim, M.-Y.; Seguin, P.; Ahn, J.-K.; Kim, J.-J.; Chun, S.-C.; Kim, E.-H.; Seo, S.-H.; Kang, E.-Y.; Kim, S.-L.; Park, Y.-J.; Ro, H.-M.; Chung, I.-M. Phenolic compound concentration and antioxidant activities of edible and medicinal mushrooms from Korea. *J. Agric. Food Chem.* **2008**, *56*, 7265–7270.

(3) FAO Statistics Division Faostat;http://faostat.fao.org/site/535/DesktopDefault.aspx?PageID=535

(4) Mohapatra, D.; Frias, J. M.; Oliveira, F. A. R.; Bira, Z. M.; Kerry, J. Development and validation of a model to predict enzymatic activity during storage of cultivated mushrooms (*Agaricus bisporus* spp.). *J. Food Eng.* **2008**, *86*, 39–48.

(5) Espin, J. C.; Jolivet, S.; Wichers, H. J. Inhibition of mushroom polyphenol oxidase by agaritine. *J. Agric. Food Chem.* **1998**, *46*, 2976–2980.

(6) Woodcock, T.; Downey, G.; O'Donnell, C. P. Review: Better quality food and beverages: The role of near infrared spectroscopy. *J. Near Infrared Spectrosc.* **2008**, *16*, 1–29.

(7) Huang, H.; Yu, H.; Xu, H.; Ying, Y. Near infrared spectroscopy for on/in-line monitoring of quality in foods and beverages: A review. *J. Food Eng.* **2008**, *87*, 303–313.

(8) Alexandrakis, D.; Downey, G.; Scannell, A. G. M. Detection and identification of bacteria in an isolated system with near-infrared spectroscopy and multivariate analysis. *J. Agric. Food Chem.* **2008**, *56*, 3431–3437.

(9) ElMasry, G.; Wold, J. P. High-speed assessment of fat and water content distribution in fish fillets using online imaging spectroscopy. *J. Agric. Food Chem.* **2008**, *56*, 7672–7677.

(10) Zhang, C.; Shen, Y.; Chen, J.; Xiao, P.; Bao, J. Nondestructive prediction of total phenolics, flavonoid contents, and antioxidant capacity of rice grain using near-infrared spectroscopy. *J. Agric. Food Chem.* **2008**, *56*, 8268–8272.

(11) Reid, L. M.; O'Donnell, C. P.; Downey, G. Recent technological advances for the determination of food authenticity. *Trends Food Sci. Technol.* **2006**, *17*, 344–353.

(12) Berrueta, L. A.; Alonso-Salces, R. M.; Héberger, K. Supervised pattern recognition in food analysis. *J. Chromatogr., A* **2007**, *1158*, 196–214.

(13) Preys, S.; Vigneau, E.; Mazerolles, G.; Cheynier, V.; Bertrand, D. Multivariate prototype approach for authentication of food products. *Chemom. Intell. Lab. Syst.* **2007**, *87*, 200–207.

(14) Blazquez, C.; Downey, G.; O'Callaghan, D.; Howard, V.; Delahunty, C.; Sheehan, E.; Everard, C.; O'Donnell, C. P. Modelling of sensory and instrumental texture parameters in processed cheese by near infrared reflectance spectroscopy. *J. Dairy Res.* **2006**, *73*, 58–69.

(15) Rutledge, D. N.; McIntyre, P. A proposed European implementation of the JCAMP-DX data file transfer format. *Chemom. Intell. Lab. Syst.* **1992**, *16*, 95–101.

(16) Barnes, R. J.; Dhanoa, M. S.; Lister, S. J. Standard normal variate transformation and de-trending of near-infrared diffuse reflectance spectra. *Appl. Spectrosc.* **1989**, *43*, 772–777.

(17) Geladi, P.; MacDougall, D.; Martens, H. Linearization and scatter-correction for near-infrared reflectance spectra of meat. *Appl. Spectrosc.* **1985**, *39*, 491–500.

(18) Savitzky, A.; Golay, M. J. E. Smoothing and differentiation of data by simplified least squares procedures. *Anal. Chem.* **1964**, *36*, 1627–1639.

(19) Davies, A. M. C.; Fearn, T. Back to basics: The "final" calibration. *Spectrosc. Eur.* **2007**, *19* (6), 15–18.

(20) Davies, A. M. C.; Fearn, T. Back to basics: Removing multiplicative effects (1). *Spectrosc. Eur.* **2007**, *19* (4), 24–28.

(21) Wold, S. Personal memories of the early PLS development. *Chemom. Intell. Lab. Syst.* **2001**, *58*, 83–84.

(22) Wold, S.; Trygg, J.; Berglund, A.; Antti, H. Some recent developments in PLS modeling. *Chemom. Intell. Lab. Syst.* **2001**, *58*, 131–150.

(23) Jørgensen, B.; Goegebeur, Y. ST02: Multivariate Data Analysis and Chemometrics. Module 7: Partial least squares regression i. http://statmaster.sdu.dk/courses/ST02/module07 (July 14, 2008).

(24) Wold, S.; Sjöström, M.; Eriksson, L. Pls-regression: A basic tool of chemometrics. *Chemom. Intell. Lab. Syst.* **2001**, *58*, 109–130.

(25) Wold, S.; Sjöström, M. Chemometrics, present and future success. *Chemom. Intell. Lab. Syst.* **1998**, *44*, 3–14.

(26) González-Arjona, D.; López-Pérez, G.; González, A. G. Performing Procrustes discriminant analysis with HOLMES. *Talanta* **1999**, *49*, 189–197.

(27) Foss NIRSystems. *Installation Manual for NIRSystems Scanning Spectrophotometers*; NIRSystems, MD, USA, 1991.

(28) Stuart, B. *Infrared spectroscopy: Fundamentals and applications*; John Wiley & Sons Ltd.: West Sussex, U.K., 2004; pp 71−93.

(29) Workman, J., *Handbook of Organic Compounds*; Academic Press: London, 2001; pp 207−242.

(30) Sánchez-Ferrer, Á.; Neptuno Rodríguez-López, J.; García-Cánovas, F.; García-Carmona, F. Tyrosinase: A comprehensive review of its mechanism. *Biochim. Biophys. Acta Protein Struct. Mol. Enzymol* **1995**, *1247*, 1–11.

(31) Prota, G. Progress in the chemistry of melanins and related metabolites. *Med. Res. Rev.* **1988**, *8*, 525–556.

(32) Hruschka, W. Data Analysis: Wavelength Selection Methods. In *Near-Infrared Technology in the Agricultural and Food Industry*, 2nd ed.; Williams, P., Norris, K. H., Eds.; AACC: St. Paul, MN, 2001.

(33) Faber, N. M.; Rajkó, R. How to avoid over-fitting in multivariate calibration--the conventional validation approach and an alternative. *Anal. Chim. Acta* **2007**, *595*, 98–106.

(34) Jolivet, S.; Arpin, N.; Wichers, H. J.; Pellon, G. *Agaricus bisporus* browning: A review. *Mycol. Res.* **2000**, *102*, 1459–1483.

(35) Chang, T.-S. Two potent suicide substrates of mushroom tyrosinase: 7,8,4′-trihydroxyisoflavone and 5,7,8,4′-tetrahydroxyisoflavone. *J. Agric. Food Chem.* **2007**, *55*, 2010–2015.

Received for review October 3, 2008. Revised manuscript received December 28, 2008. Accepted January 8, 2009. Financial support from the Irish Department of Agriculture, Fisheries and Food under the FIRM Program is gratefully acknowledged. C.E. is a Teagasc Walsh Fellow.

JF803090C